Somatic maintenance alters selection acting on mutation rate

Authors:

Andrii I. Rozhok[1] and James DeGregori[1,2,3,4]

[1]Department of Biochemistry and Molecular Genetics, [2]Integrated Department of Immunology, [3]Department of Pediatrics, [4]Department of Medicine, Section of Hematology, University of Colorado School of Medicine, Aurora, CO 80045

Corresponding Authors:

Andrii I. Rozhok: Andrii.Rozhok@ucdenver.edu

James DeGregori: James.DeGregori@ucdenver.edu

Acknowledgments

We would like to thank Mark Johnston, L. Alex Liggett and David Pollock of the University of Colorado, and Robert Gatenby and Andriy Marusyk of the Moffitt Cancer Center for critical review of the manuscript. These studies were supported by National Cancer Institute grant R01CA180175 to J.D.

Abstract

The evolution of multi-cellular animals has produced a conspicuous trend toward increased body size. This trend has introduced at least two novel problems: an elevated risk of somatic disorders, such as cancer, and declining evolvability due to reduced population size, lower reproduction rate and extended generation time. Low population size is widely recognized to explain the high mutation rates in animals by limiting the presumably universally negative selection acting on mutation rates. Here, we present evidence from stochastic modeling that the direction and strength of selection acting on mutation rates is highly dependent on the evolution of somatic maintenance, and thus longevity, which modulates the cost of somatic mutations. We propose a theoretical model for how evolvability and germline mutation rates can be under positive selection in sexually reproducing organisms by their co-selection with adaptive alleles that overcomes gene segregation produced by genetic recombination. We argue that this mechanism may have been critical in facilitating animal evolution.

Keywords: somatic maintenance, longevity, body size, mutation rate, selection

Introduction

Increasing body size has been one of the major trends in animal evolution across many taxa, as formulated in Cope's rule (Heim et al., 2015, Baker et al., 2015). The evolution of larger bodies introduces some fundamentally new evolutionary challenges. The carrying capacity of ecosystems limits biomass per group/species, so larger body size leads to reduced population size. Furthermore, large animals generally demonstrate lower reproduction rates and longer generation times. In aggregate, such changes weaken selection that can act on a population and thus negatively affect evolvability. This general reduction in evolvability should, however, be at least partially alleviated by diversity facilitated by sexual reproduction.

The mutation rate (MR) is another critical evolvability parameter. It is believed that selection generally acts to lower MR (Kimura, 1967, Baer et al., 2007, Dawson, 1999), and the significantly higher MRs observed in animals compared to unicellular organisms have been argued to result from the reduced power of selection imposed by small population sizes (Lynch, 2010, Lynch, 2011, Lynch et al., 2016). Germline (gMR) and somatic (sMR) mutation rates are linked, as they employ the same basic DNA replication and repair machinery (Pothof et al., 2003, Marcon & Moens, 2005, Galetzka et al., 2007). While elevated gMR improves evolvability, the ensuing higher sMR should elevate the risk of somatic disorders, such as cancer (Hanahan & Weinberg, 2000). For cancer, increasing body size is expected to increase the frequency of oncogenic mutations by increasing the number of target cells (Caulin & Maley, 2011). Somatic mutations also contribute to aging and a variety of aging-related diseases (Lopez-Otin et al., 2013). The increased cost of sMR should thus exert negative selective pressure on gMR in larger animals.

Recent evidence demonstrates that the sMR in some animal tissues can be significantly higher than the rate inferred from observed mutations, because somatic purifying selection is very effective in eliminating damaged somatic cells (Pfau et al., 2016). Many mechanisms, such as various tumor suppressor gene functions (including DNA damage induced apoptosis) (Sherr, 2004), autophagy (Glick et al., 2010), purifying somatic selection (Pfau et al., 2016, Rozhok & DeGregori, 2016), and immune surveillance (Swann & Smyth, 2007), should buffer the costs of

65 somatic mutation and in aggregate promote lifespan extension by maintaining tissue integrity.
66 We will collectively call these mechanisms – the *somatic maintenance program* (SMP).

67 We present theoretical evidence from Monte Carlo modeling indicating that somatic
68 maintenance not only improves individuals' survival for large animals by reducing sMR costs,
69 but should have played a crucial role in animal evolution by substantially modifying selection
70 acting on gMR. We show that positive selection for increased body size promotes positive
71 selection for extended longevity by improving SMP. Our results also indicate that positive
72 selection on traits that do not impact somatic risks also promotes selection for an improved SMP.
73 In both cases, positive selection on gMR was observed because of the reduced sMR cost, which
74 dramatically improved evolvability of the simulated population. While high MR is always a
75 disadvantageous trait on its own, we propose a model for how MR contributes to individual net
76 fitness and how small population size promotes selection for higher evolvability by elevating
77 gMR.

78

79 **Methods**

80 **Software.** The model was created and all simulations were run in the Matlab environment
81 (MathWorks Inc, MA) version R2014a.

82 **Model algorithm.** The model is a stochastic Monte Carlo type model (the exact algorithm can be
83 found in **Supplements: Section 1a**) that runs a total of 1,005,000 updates ("time" in arbitrary
84 units, AU) unless otherwise stated, which represents ~1000 generations of the simulated animal
85 population. The simulation starts with building an initial population of 10,000 individuals. Each
86 individual has a number of simulated traits: 1) ID, which is 1 (monogenotypic population) or 1
87 and 2 (in experiments with competition between two genotypes in a mixed population to indicate
88 genotypes); 2) current age, which increments by 1 at each simulation update; 3) inherited body
89 mass, which is inherited with variation by an individual and will be reached by adulthood (at age
90 ~1000) and equals 5000 AU in the initial population; 4) current body mass, which changes during
91 individual growth, following a growth curve, and plateaus at the inherited body mass in adults;
92 5) inherited birth mass, which in individuals of the initial population is 300 AU; 6) inherited

mutation rate of 10^{-9} AU (explained below); 7) inherited reproduction rate, which is the period with variation between successive reproductions in adult individuals and equals ~600 in the initial population; 8) inherited litter size (initially 1), which is the number of progeny produced per individual per reproduction; 9) inherited parameter of somatic maintenance, which determines the strength of the somatic maintenance program as further explained below; 10) age of first reproduction, which dictates that an individual begins reproducing when its current body mass reaches 0.9693 of its inherited adult body mass (the number is derived so that in the initial population maturity is reached at age ~1000 based on the growth curve).

Each inherited trait varies in progeny relative to parental. This variation was produced by multiplying the inherited mutation rate by the parameter of inherited variance (*inhvar* = 250,000,000) and the product was used as the standard deviation (STD) of the normally distributed variation in inheritance. This transformation was not necessary, as the *inhvar* parameter is constant throughout simulation and it simply determines the magnitude of the mutation rate's effects in germline, which is imaginary and in the initial population simply produces 0.000000001 x 25,000,000 = 0.025 that serves as the STD parameter for the normal distribution from which inheritance variation is drawn. However, we kept this two-parametric model for inheritance because mutation rate is also separately used in the equation of the somatic maintenance program (as will be explained later).

Each newborn individual grows, reaches maturity, then reproduces over the rest of its lifetime and eventually dies. The model is asynchronous, so that at every time-point of the simulation the population contains individuals of various ages whose lifecycles develop independently. The model operates with single-parent reproduction model so that each individual descends from one parent. In this regard, technically it is tempting to view it as a model of an asexual population. However, at a higher level of abstraction the fundamental difference between sexual and asexual populations (aside from the issue of purging deleterious mutations) is the amount of variation produced per the same size population per generation. Variance of inheritance in our model (as shown above) is obviously too high to be assumed as being generated by mutations accumulating along a clonal lineage and equals 10% of a trait's value per generation within 95 percentile. As the modeled traits are assumed to be *multigenic* and have a continuous phenotypic range in the population, we did not need to simulate the processes of allelic

segregation by recombination in order to reconstruct a sexual population. As such, the model only operates with the net ultimate change of a trait over generations. At this level of abstraction, the effective difference between a sexual and asexual population is reduced to the amount of variation in phenotypically manifested inheritance per population size per generation. We account for population size in this definition by inferring that this variance per se will not depend on population size, but larger populations will have higher chance of generating extreme phenotypes, e.g. those beyond 95 percentile on a per generation basis.

And finally, three factors of mortality were modelled in the simulations. First, at every timepoint of the simulation, an individual could die of somatic causes with a certain probability. This probability is small at the beginning of life (but still can be caused by some imaginary inherited genetic defects) and increases exponentially with age based on the paradigm of the aging curve, which is primarily determined by an individual's inherited somatic maintenance program (SMP). In humans, the aging curve also depends on lifestyle, however we assume in this model that in a wild animal population lifestyle distribution is sufficiently uniform to be neglected. More detailed description of the somatic maintenance paradigm we applied will be explained further below. Secondly, the simulated animals had a chance of dying of external hazards, such as predators. We applied the Lotka-Volterra model of predator-prey interactions (Lotka, 1925, Volterra, 1926) to implement the dynamics of predator pressure (effectively the chance of dying of an external hazard cause per timeunit). Here we should mention that smaller individuals and juveniles had higher chances of dying of external hazards, which effectively created positive selection for body size and also reflected the typical high mortality rates among juveniles observed in natural populations. And lastly, individuals could die of intra-specific competition. We implemented such competition by setting the upper limit of population's total biomass, which in nature is imposed by the ecosystem's carrying capacity. Therefore, in the simulated population biomass produced over the biomass limit caused additional mortality so that stochastically population total biomass never exceeded the limit. Larger individuals also had lower probability of dying of intra-specific competition, based on the assumption that competition for resources and mates (the failure to reproduce is effectively an evolutionary death) will typically favor larger individuals and this should have been one of the forces that has been driving the macroscopic animal evolutionary trend towards increasing body size. The advantage of size in this mortality model also created

153 additional positive selective pressure for body size. The total age-dependent mortality of all
154 causes in our model did approximate a typical wild animal mortality curve (**Supplements: Section**
155 **3**).

156 **The somatic maintenance program paradigm.** In order to replicate natural mortality caused by
157 physiological aging, such as cancer, decreased immune defense and lower ability to avoid
158 predators or to succeed in intra-specific competition, we made use of the aging curve, or somatic
159 maintenance, concept. Modern humans (in developed nations) and captive animal mortality
160 curves (**Fig. 1B** for human) differ from wild animal mortality curves in very high early life survival
161 with most mortality significantly delayed into advanced ages (Hochberg & Noble, 2017, Madsen
162 et al., 2017). This difference is caused by many reasons, such as much lower mortality caused
163 by external hazards and better nutrition and general healthcare. It therefore can be assumed
164 that the human and captive animal mortality curves are close representations of the physiological
165 aging curve. As longevity depends on multiple mechanisms of maintaining the soma, we can
166 also call this curve *the somatic maintenance curve*. In order to reconstruct this curve, we
167 assumed that somatic maintenance depends on the interaction of two opposing forces: 1) the
168 accumulation of genetic and structural damage in the soma that promotes aging and 2) the
169 somatic maintenance program consisting of a number of mechanisms that prevent or buffer the
170 effects of genetic and structural damage. The exact mathematical relationship between these
171 two forces and age is not known, however an example of cancer development can be used as
172 a proxy to explain the equation we derived for it. Oncogenic mutations (including oncogenic
173 epigenetic changes) are the ultimate necessary condition for cancer to develop. The frequency
174 of oncogenic mutations linearly depends on mutation rate on a per cell division basis. Therefore,
175 we assume that linear changes in mutation rate will have linear effects on the odds of the
176 occurrence of oncogenic mutations. An oncogenic mutation provides the initiated cells with a
177 linear change in their fitness relative to normal cells. However, over time an advantageous clone
178 with a constant linear fitness advantage will proliferate exponentially. Therefore, we can already
179 assume that mutation rate should have a linear effect on the cancer curve, while time/age adds
180 an exponential component revealed in an exponential growth of a tumor. We can reasonably
181 assume further that a strong SMP will efficiently suppress such a clone, slowing or even
182 preventing its growth. A weaker SMP will allow the clone to proliferate faster. Therefore, SMP

183 strength can modulate the effects of mutations and time on cancer risk. The exact relationship
184 between SMP strength and physiological risk factors is not known. However, we know that their
185 interaction leads to a net exponent in physiological decline and disease risk. We therefore
186 reconstructed the human aging curve by maintaining the general principal relationship between
187 these factors as shown in **Eq. 1**. As seen from the equation, mutation rate is a linear contributor
188 to aging. Age itself contributes exponentially, and the somatic maintenance composite
189 parameter *Som* is, in turn, in power relationship to age. The cumulative distribution function of
190 D_A (**Eq. 1**) produces *D(A)* – the probability of dying of somatic/physiological causes by age *A* and
191 yields a shape close to the human mortality curve (**Fig. 1A,B**). We cannot claim that these three
192 factors are in the exact relationship predicted by **Eq. 1**, as it is unknown. As seen in **Fig. 1A**,
193 changes in the *Som* parameter have substantially greater effects on the resulting mortality curve
194 than mutation rate, with mutation rate still having a sizeable effect as well. Yet claims are still
195 made(Kennedy et al., 2012) that mutation rate is a larger factor in aging than we assume in this
196 model. Validation of our assumption in general comes from the body of solid evidence that up to
197 50% of mutations in humans accumulate during body growth by the age 18-20 (Finette et al.,
198 1994, Giese et al., 2002, Horvath, 2013). If mutation accumulation had a significant effect on
199 aging on its own, we should age rapidly until age 18-20 (half-way) and then the rate of aging
200 should decelerate. However, in reality the opposite happens, indicating that the combined
201 strength of the SMP has an overpowering effect in modulating the effects of genetic damage on
202 aging. As a result, we reason that **Eq. 1** might reasonably approximate the natural relationships
203 of these three factors. Therefore, based on an individual's aging curve we calculated the D_A
204 parameter at each simulation time-point (using the individual's mutation rate, age and *Som*
205 parameter) and applied it in a binomial trial as the probability of that individual's dying of
206 somatic/physiological causes in an age-dependent manner. As further explained in
207 **Supplements: Section 4**, the exact relationship between the *Som* parameters and each of the
208 other two (mutation rate and age) has no effect on the model, as the model represents SMP and
209 its variation by using area under the mortality curve, therefore the sole purpose of **Eq. 1** in the
210 model is to generate an age-dependent curve of physiological mortality whose cumulative
211 function (probability of dying by a certain age) resembles in shape the human mortality/aging
212 curve (see **Supplements: Section 4** for detailed explanation and illustration).

Model variations. A number of model variations used in simulation experiments are employed. *Fixed trait values* involved simply fixing the initial trait value without inherited variation throughout the entire simulation. *Dislinking of somatic and germline mutation rate* was done by making the value *M* in **Eq. 1** independent of an individual's mutation rate, which resulted in somatic costs independent of transgenerational variation of mutation rate (effectively from germline mutation rate). *Selection for a trait that did not affect somatic risks* was achieved by transforming the "body mass" trait's effects by removing the trait from calculations of the risk of death by somatic causes (unlike body size, it did not influence the risk), then removing the population biomass limit and setting maximum population size (unlike body mass, other traits do not directly affect population numbers) and fixing the growth rate curve so that it reached the initial body mass of 5,000 AU (the current body mass parameter in the model; the inherited body mass variation did not exist and the inherited body mass parameter was replaced with the somatic risk unrelated trait). These manipulations made the selected trait a proxy for a trait unrelated to somatic risks (e.g. hair color). *Competitive assays* included individuals with different ID parameters, such as 1 and 2 to indicate different "genotypes"; traits of the "genotypes" then were tracked and stored separately.

Data processing. Processing of primary data included removal of outliers (see **Supplements: Section 5**). Occasionally the simulations generated "NaN" (not a number) values in individual parameters, which were rare but quickly propagated if left in the population. We immediately deleted individuals from the population if "NaN" values appeared in any of their parameters. Based on the rarity of such events, we can assume that they had the effect of rare early lethal mutations and affected the population at random. Thus we assume these did not affect the principal results.

Statistics and data presentation. Most simulation experiments were made with 25 repeats. Due to heavy skews in sample distributions (inferred by D'Agostino-Pearson test for normality of a distribution), all figure panels represent medians (thick lines) and 95 percentiles on each tail (color-shaded areas). Statistical differences between experimental conditions were calculated as follows. We first calculated the sum of all values in each run throughout the entire evolution

241 of a trait (typically 1,005,000 time points). In this way, given the small increment over a long time
242 the sum essentially approximated the area under the curve of a trait's evolution. These sums
243 (usually 25 repeats in one experiment/sample) were then compared by applying the Matlab
244 implementation of the Wilcoxon rank sum test, which is considered equivalent to the Mann-
245 Whitney U-test. P-values <= 0.05 were considered as indicating significant difference.

246

247 **Results**

248 We built a stochastic model of evolution in animal populations, incorporating reproduction
249 and survival, whereby each individual's traits are inherited with variance proportional to gMR (for
250 code, see **Supplements: Section 1a**). Traits are assumed to be polygenic and exhibit phenotypic
251 variation in the population. The evolution of body size, somatic maintenance and germline
252 mutation rate was then tracked under various regimens of selection. The model reasonably
253 approximates a sexually reproducing population as explained in **Methods: Model algorithm**.

254 The model incorporates three major factors of mortality, including aging. Human life tables
255 indicate that aging proceeds exponentially, whereby mortality and diseases accelerate at
256 advanced ages (e.g. https://www.ssa.gov, https://seer.cancer.gov). The combined action of
257 SMP mechanisms provides for an extended early period of high body fitness with little to no
258 decline. We generalized this complex program in a curve that describes modeled animal
259 mortality of physiological causes schematically shown in **Fig. 1A** and based on the following
260 equation:

261 $$D_A = M \times e^{A^{Som}} \qquad (1)$$

262 where D_A is the probability of dying of physiological causes at age A, M is mutation rate, and
263 *Som* is a composite parameter that determines SMP efficiency. The cumulative distribution
264 function of D_A, or the probability of dying of physiological causes by age A, resembles human
265 mortality (**Fig. 1B**). The equation should thus provide a robust model for aging-related mortality,
266 reflecting the extended period of high fitness and the late-life accelerating mortality. **Fig. 1A** also
267 demonstrates the relative effects of MR, which is a linear contributor, and the *Som* parameter,

268 which stands for the total damage buffering capacity of the SMP (for details and theory see
269 **Methods: The somatic maintenance program paradigm**). It is important to keep in mind that the
270 *M* parameter (mutation rate) in **Eq. 1** is responsible for the somatic costs of MR (higher MR in
271 **Fig. 1A** accelerates aging-related mortality).

272 In our simulations, positive selection for body size (**Fig. 1C, green**) led to a concurrent
273 selection for elevated gMR (**Fig. 1D, green**) and improved SMP (**Fig. 1E, green**). Artificially
274 blocking SMP evolution by fixing SMP at the initial value (**Fig. 1E, blue**) significantly slowed the
275 evolution of body size (**Fig. 1C, blue; $p << 0.001$**) and triggered negative selection on gMR (**Fig.**
276 **1D, blue**). We implemented the ecosystem carrying capacity by setting a maximum biomass for
277 the population; therefore, increasing body size led to a corresponding decline in population
278 numbers, amplifying the power of drift (**Fig. 1F,G**). When SMP was allowed to evolve, however,
279 the population entered a "drift zone" when its size decreased to ~4,000 individuals, which shortly
280 thereafter was overcome by selection for even larger body size, visible also by a continuing
281 decline in population numbers (**Fig. 1F**). When we artificially blocked SMP, however, the drift
282 zone was more profound. It occurred earlier at the population size of ~6,000-7,000 individuals,
283 and the population was not able to escape from it (for ~1,000 generations) and restore its initial
284 rates of evolution (**Fig. 1G**), indicating an important role of SMP evolution in maintaining
285 evolvability. We further generated a population with two simulated genotypes – Genotype A that
286 could evolve SMP (10% of the population) and Genotype B with SMP fixed at the initial value
287 (90%). We set a maximum population size and removed the maximum biomass limit to rule out
288 body mass effects on population size and selection, and tracked Genotype A and Genotype B
289 frequencies under positive selection for body size (for code see **Supplements: Section 1b**).
290 Despite the initial abundance, Genotype B (with fixed SMP) lost the competition in less than 200
291 generations, reflecting a direct competitive advantage of the capacity to evolve enhanced SMP
292 (**Fig. 1H**). Hereafter, we will call the setting with positive selection for body size and freely
293 evolving SMP and gMR the *standard condition* (usually shown in green, unless otherwise
294 indicated) used in comparisons with other selection regimens.

295 In the absence of positive selection for increased body mass (**Fig. 2A, blue**), both gMR (**Fig.**
296 **2B, blue**) and SMP (**Fig. 2C, blue**) demonstrate early positive selection, which appeared to have
297 been caused by rapid evolution of reproductive parameters (see **Supplement: Section 2**).
298 Overall, gMR demonstrates a significant general decrease (non-overlapping confidence
299 intervals (CIs) at the beginning relative to the end of the simulation), and SMP undergoes a
300 significantly smaller improvement compared to the standard condition (green; $p \ll 0.001$).
301 Blocking the evolution of body mass (**Fig. 2D, blue**) and SMP (**Fig. 2F, blue**) expectedly led to
302 strong selection for lower gMR (**Fig. 2E, blue**) compared to the standard condition ($p \ll 0.001$),
303 which we interpret as being driven by the sMR costs in the absence of benefits of high gMR. In
304 other words, mutation rate is selected against because of its somatic costs and the absence of
305 benefits of higher gMR in static conditions. In natural populations that are under stabilizing
306 selection, gMR will have costs due to greater phenotypic variance from a well-adapted state that
307 are independent of sMR, but we do not model stabilizing selection in this study.

308 To investigate the role of the putative gMR benefit versus sMR cost balance in evolution,
309 we further decoupled gMR and sMR by allowing gMR to evolve but making sMR cost fixed and
310 independent of gMR (see **Methods: Model variations**). Decoupling sMR cost from gMR
311 significantly accelerated the evolution of body size (**Fig. 2G, blue**) relative to the standard
312 condition (green; $p = 0.0052$), revealing that sMR costs can limit the evolution of larger body
313 size. During the early fast evolution of body mass, gMR (**Fig. 2H, blue**) and SMP (**Fig. 2I, blue**)
314 demonstrate a corresponding positive response. Later, further body mass evolution becomes
315 impeded (likely because of the severe depletion in population numbers), coinciding with
316 selection against gMR. SMP plateaus during this second phase at a significantly lower level
317 compared to the standard condition ($p \ll 0.001$), indicating that the somatic costs of mutation
318 rate stimulate the evolution of more robust SMP.

319 As we have seen under blocked selection for body size (**Fig. 2B,C, blue**), SMP demonstrates
320 an early phase of positive selection (**Fig. 2C, blue**) that is apparently reflected in a corresponding
321 positive selection for gMR (**Fig. 2B, blue**). This observation suggests that both SMP and gMR
322 may also respond to selection acting on some other traits, e.g. reproductive parameters

323 (**Supplements: Section 2**). This raises the question whether SMP and gMR evolution would be
324 sensitive to strong selection for a trait that does not affect somatic risks (greater body size
325 increases the target size for somatic mutations). We simulated a condition that was similar to
326 the standard condition, except positive selection was applied to a trait that did not affect sMR
327 related somatic costs (see **Methods: Model variations**); e.g. if SMP improvement is solely a
328 response to the increased sMR cost imposed by larger body, selection for an sMR cost unrelated
329 trait should not drive improvements in SMP. As shown in **Fig. 2J (blue)**, unimpeded by increased
330 sMR costs and declining population size, the evolution of an sMR cost unrelated trait is
331 significantly faster compared to the evolution of increased body size ($p << 0.001$). Interestingly,
332 gMR (**Fig. 2K, blue**) also demonstrated an early phase of positive selection during early rapid
333 evolution of the selected trait and remains above the initial gMR throughout the entire simulation.
334 As anticipated, SMP is positively selected, however in the absence of an increasing sMR cost
335 (associated with larger bodies), SMP's improvement is significantly smaller (**Fig. 2L, blue,** $p <<$
336 0.001). Notably, even with much less enhanced SMP, gMR is still under positive selection in
337 response to positive selection of the sMR cost unrelated trait (**Fig. 2L, blue**), consistent with the
338 sMR/gMR cost/benefit ratio being an important factor regulating selection acting on gMR.
339 Regardless, the results demonstrate that both gMR and SMP are responsive to selection for
340 somatic risk unrelated traits, which indicates that high mutation rate is beneficial in positively
341 selective conditions.

342 As we have seen in **Fig. 2D-F**, in the absence of strong positive selection for body size and
343 SMP efficiency, selection acts to lower gMR. **Fig. 3** shows, however, that this selection is
344 significantly modified by the efficiency of SMP. Stronger SMPs (lower *Som* value) relax selection
345 for lower gMR when directional selection is weak (non-overlapping CIs between the standard
346 (red) and either of the improved SMPs). As will be explained further below, this observation may
347 have significant implication on long-term species survival.

348 Under strong positive selection, whether for body mass (**Fig. 1A-C, blue**) or a sMR cost
349 unrelated trait (**Fig. 2H,I, blue**, and **Fig. 2K,L, blue**), gMR demonstrates consistent signs of
350 positive selection. However, because gMR and sMR are linked, higher gMR is a trait that should

negatively impact individual fitness and therefore be under negative selection. To investigate this question, we mixed two simulated genotypes, one “wild-type” (50%) and one “mutator” (50%) in a population of stable size and under positive selection for a sMR cost unrelated trait. We then observed the genotypes’ frequencies in the population using varying strength of mutators. **Fig. 4A** demonstrates that while the mutator’s fitness initially is lower compared to wild-type, eventually the mutator outcompetes its wild-type counterpart. Interestingly, with increased mutation rate, the magnitude of the mutator’s initial decline increases, but so does the speed at which it subsequently overtakes the population. This result provides a clue for how higher mutation rate, being a trait with negative impact on fitness, can be selected for. Because net organismal fitness is a composite trait impacted by the fitness value of many individual traits, the initial fitness of the “mutator” is lower because, all other traits equal, higher MR incurs increased sMR cost. However, in response to selection, mutator is capable of more rapidly developing other (adaptive) traits (**Fig. 4B**) and thus its overall fitness soon becomes higher compared to wild-type. Its noteworthy that genetic recombination in sexually reproducing populations should theoretically act to segregate adaptive alleles (under positive selection) from mutator alleles that are not directly selected for and even should be negatively selected. **Fig. 5** shows a model that we propose to explain how small population size should effectively impede such allelic segregation under positive selection. Importantly, **Fig. 5** also demonstrates that higher gMR is only beneficial under positive selection, while stabilizing selection will act to lower it even in the absence of the incumbent somatic risks.

Discussion

Our study demonstrates that positive selection for body size triggers a concurrent selection for improved somatic maintenance to mitigate the increased somatic risks of larger bodies. Improved somatic maintenance, in turn, promotes selection for higher germline mutation rates by reducing the cost of somatic mutations and thus altering the sMR/gMR cost/benefit ratio. Conditions of strong positive selection for other than SMP traits, as our model shows, can also

alter this balance by elevating the benefits of higher gMR. Under stable conditions, alternatively, the sMR/gMR cost/benefit balance is altered by the existing cost of somatic mutations and by the increased cost and absent/reduced benefits of gMR itself (as shown in **Fig. 5A**), which ultimately favors lower mutations rates. Under stasis, gMR exerts a cost independent of somatic risks by increasing deviation of progeny phenotypes from population mean/median and thus reducing their fitness. Our study thus demonstrates that the evolution of mutation rate is not exclusively limited by negative selection and population size, but is highly tunable and governed by selection acting on other traits. Importantly, our modeling indicates that under certain conditions elevated mutation rate, unlike perhaps any other trait, can be positively selected despite its negative effects on individual fitness (as explained in **Fig. 4**). Mutation rate, therefore, does not entirely fit in the paradigm formulated by George C. Williams (Williams, 1966) that evolution does not have eyes for the future (which appears universal for other traits). Being maladaptive in stable conditions, higher mutation rate becomes a trait that improves the net multi-trait fitness in conditions of positive selection for other traits by generating greater diversity of other traits, thus increasing a population's sensitivity to selection and accelerating adaptation. These observations can provide an explanation why mutation rate, although showing some major patterns, neither strictly follows phylogeny nor population size in mammals as shown by Lynch (Lynch, 2010).

Mutation rate in eukaryotes is a highly polygenic trait encoded by multiple genes involved in DNA replication, repair and cell division machineries (Pothof et al., 2003, Galetzka et al., 2007). Animals mostly reproduce sexually, which should generate an extensive population allelic diversity for these genes. This diversity should provide for a relatively continuous distribution of mutation rate in populations, rather than being a uniform trait marked with sporadic monogenic mutants, as may occur in asexual populations (Cox & Gibson, 1974, Gibson et al., 1970, Sniegowski et al., 1997). Such intra-population variation (Harris, 2015, Conrad et al., 2011), as well as the ability of mutation rate to rapidly evolve (Harris & Pritchard, 2017), has been shown for humans . However, sexual reproduction would be supposed to effectively segregate alleles contributing to mutation rate from alleles for other (e.g. adaptive) traits. It has been argued based

406 on other evidence that the efficiency of such segregation in sexual populations is limited (Draghi
407 & Wagner, 2008). Here, we argue that given the polygenic nature of mutation rate, such
408 segregation should be much less efficient in small populations that are under positive selection,
409 and should be substantially impeded by selection for extreme phenotypes (as shown in **Fig. 5**).
410 The polygenic nature of mutation rate should also impede segregation of mutator phenotypes
411 from adaptive phenotypes, as most genes contributing to the overall mutation rate will
412 individually have rather modest effects on fitness and in many cases their effect on fitness may
413 depend on the allelic composition of other loci. In monogenic traits, on the other hand, a single
414 locus will have a defined effect on the net phenotype and thus will directly affect selection acting
415 on it.

416 It also appears from our results that animal evolution, with the macroscopic trend toward
417 larger bodies, should have driven a concurrent evolution of extended longevity, the latter being
418 determined by the efficiency of species-specific somatic maintenance programs. Even though
419 extended longevity tentatively appears to be a benefit on its own, e.g. due to extended
420 reproduction period, our model demonstrates that somatic maintenance (and thus longevity) is
421 under a much weaker positive selection in the absence of other positively selected traits. This
422 observation can explain why extended longevity demonstrates significant deviations across
423 animal taxa from the general rule larger body → longer lifespan. Our results indicate that the
424 evolution of longevity (as a function of somatic maintenance efficiency) should be greatly
425 impacted by the rate of evolution of other traits, and not necessarily body size.

426 Interestingly, our study predicts an important evolutionary role for the mechanisms of
427 somatic maintenance in addition to their evolution as a means of improving individual survival of
428 large animals (Caulin & Maley, 2011, Rozhok & DeGregori, 2016). Our results demonstrate that
429 selection for enhanced somatic maintenance goes well beyond the evolution of body size and is
430 promoted by strong directional selection acting on any trait. This result indicates that SMPs may
431 have had an important role in the evolution of large animals. Selection for higher gMR ensuing
432 improved SMP may be an important mechanism "rescuing" the reduced evolvability imposed by
433 reduced population size, extended generation times and lower reproduction rates. Therefore,

434 SMPs and longevity may have an important contribution to species long-term survival. For
435 example, a prolonged evolutionary stasis (Benton & Pearson, 2001, Eldredge & Gould, 1972,
436 Gould & Eldredge, 1993, Venditti et al., 2011) should trigger selection for lower mutation rates.
437 By relaxing negative selection on mutation rate and thus maintaining evolvability (as shown in
438 **Fig. 3**), enhanced SMPs can ensure better survival of animal groups facing rapid evolutionary
439 transitions or drastically changed environments after such relatively static periods. All other traits
440 equal, species with extended longevity may survive such transitions with higher probabilities.

441 Lynch and colleagues have provided extensive arguments supporting the idea that the
442 higher MRs in animals compared to unicellular organisms are likely to be caused by reduced
443 population sizes that limit the ability of negative selection to act on mutation rate (Lynch, 2010,
444 Lynch, 2011, Lynch et al., 2016). In conjunction with population size, in large animals the
445 strength of selection will be further attenuated by lower reproduction rates and extended
446 generation times. Based on our results, Lynch's theory can be extended by recognizing that
447 somatic maintenance programs (and longevity) should have substantial influence on the general
448 relationship between population size and mutation rates, and on the strength and directionality
449 of selection acting on mutation rates. For example, in our simulation, populations of the same
450 initial size but with different SMP efficiencies demonstrate profound differences in the effects of
451 population size driven weakening of selection (**Fig. 1F,G**, as well as discrepant selection for
452 mutation rates (**Fig. 1D**).

453 Selection for higher mutation rates has been shown experimentally in bacteria (Gibson et
454 al., 1970, Cox & Gibson, 1974, Sniegowski et al., 1997, Loh et al., 2010), whereby engineered
455 or spontaneous mutants with higher mutation rate have been shown to have advantages over
456 wild-type in positively selective conditions. The "mutator hitchhiker hypothesis" explains such
457 selection by the higher probability that adaptive mutations will appear in a mutator cell
458 (Sniegowski et al., 1997). Once such a mutation occurs, the mutator genotype spreads to fixation
459 by being genetically linked to the adaptive phenotype. Modeling studies demonstrate that
460 evolution of evolvability, including varying selection on mutation rates, should be possible in

sexually reproducing organisms (Jones et al., 2014, Draghi & Wagner, 2008, Jones et al., 2007). Yet robust experimental corroboration of such a possibility appears to be lacking.

In conclusion, our results raise the question of whether the evolution of large body size in animals would be possible without such a complex pattern of selection acting on mutation rate, and whether such a complex relationship is necessary to explain the evolution of large animals. The evolution of large bodies has entailed the cost of losing the ability to evolve via all major parameters that define this ability, such as population size, reproduction rate and generation time, <u>except</u> mutation rate (which increased). Therefore, one scenario could have been that this cost has been so prohibitive for many species that positive selection for mutation rate was necessary to allow evolution of large animals. Alternatively, mutation rate could have been high enough to maintain evolvability at the negative selection/drift barrier point where negative selection was no longer able to reduce it further (Lynch, 2010). Understanding which of these scenarios prevails in the evolution of large animals requires more research.

477 ## References

478 Baer, C. F., Miyamoto, M. M. & Denver, D. R. 2007. Mutation rate variation in multicellular eukaryotes: causes
479 and consequences. *Nat Rev Genet* **8**: 619-31.
480 Baker, J., Meade, A., Pagel, M. & Venditti, C. 2015. Adaptive evolution toward larger size in mammals. *Proc Natl*
481 *Acad Sci U S A* **112**: 5093-8.
482 Benton, M. J. & Pearson, P. N. 2001. Speciation in the fossil record. *Trends Ecol Evol* **16**: 405-411.
483 Caulin, A. F. & Maley, C. C. 2011. Peto's Paradox: evolution's prescription for cancer prevention. *Trends Ecol Evol*
484 **26**: 175-82.
485 Conrad, D. F., Keebler, J. E., DePristo, M. A., Lindsay, S. J., Zhang, Y., Casals, F., Idaghdour, Y., Hartl, C. L., Torroja,
486 C., Garimella, K. V., Zilversmit, M., Cartwright, R., Rouleau, G. A., Daly, M., Stone, E. A., Hurles, M. E. &
487 Awadalla, P. 2011. Variation in genome-wide mutation rates within and between human families. *Nat*
488 *Genet* **43**: 712-4.
489 Cox, E. C. & Gibson, T. C. 1974. Selection for high mutation rates in chemostats. *Genetics* **77**: 169-84.
490 Dawson, K. J. 1999. The dynamics of infinitesimally rare alleles, applied to the evolution of mutation rates and
491 the expression of deleterious mutations. *Theor Popul Biol* **55**: 1-22.
492 Draghi, J. & Wagner, G. P. 2008. Evolution of evolvability in a developmental model. *Evolution* **62**: 301-15.
493 Eldredge, N. & Gould, S. J. (1972) Punctuated equilibria: an alternative to phyletic gradualism. In: *Models in*
494 *Paleobiology*, (Schopf, T. J. M., ed.). pp. 82-115. Freeman Cooper, San Francisco.
495 Finette, B. A., Sullivan, L. M., O'Neill, J. P., Nicklas, J. A., Vacek, P. M. & Albertini, R. J. 1994. Determination of
496 hprt mutant frequencies in T-lymphocytes from a healthy pediatric population: statistical comparison
497 between newborn, children and adult mutant frequencies, cloning efficiency and age. *Mutat Res* **308**:
498 223-31.
499 Galetzka, D., Weis, E., Kohlschmidt, N., Bitz, O., Stein, R. & Haaf, T. 2007. Expression of somatic DNA repair genes
500 in human testes. *J Cell Biochem* **100**: 1232-9.
501 Gibson, T. C., Scheppe, M. L. & Cox, E. C. 1970. Fitness of an Escherichia coli mutator gene. *Science* **169**: 686-8.
502 Giese, H., Snyder, W. K., van Oostrom, C., van Steeg, H., Dolle, M. E. & Vijg, J. 2002. Age-related mutation
503 accumulation at a lacZ reporter locus in normal and tumor tissues of Trp53-deficient mice. *Mutat Res*
504 **514**: 153-63.
505 Glick, D., Barth, S. & Macleod, K. F. 2010. Autophagy: cellular and molecular mechanisms. *J Pathol* **221**: 3-12.
506 Gould, S. J. & Eldredge, N. 1993. Punctuated equilibrium comes of age. *Nature* **366**: 223-7.
507 Hanahan, D. & Weinberg, R. A. 2000. The hallmarks of cancer. *Cell* **100**: 57-70.
508 Harris, K. 2015. Evidence for recent, population-specific evolution of the human mutation rate. *Proc Natl Acad*
509 *Sci U S A* **112**: 3439-44.
510 Harris, K. & Pritchard, J. K. 2017. Rapid evolution of the human mutation spectrum. *Elife* **6**.
511 Heim, N. A., Knope, M. L., Schaal, E. K., Wang, S. C. & Payne, J. L. 2015. Animal evolution. Cope's rule in the
512 evolution of marine animals. *Science* **347**: 867-70.
513 Hochberg, M. E. & Noble, R. J. 2017. A framework for how environment contributes to cancer risk. *Ecol Lett* **20**:
514 117-134.
515 Horvath, S. 2013. DNA methylation age of human tissues and cell types. *Genome Biol* **14**: R115.
516 Jones, A. G., Arnold, S. J. & Burger, R. 2007. The mutation matrix and the evolution of evolvability. *Evolution* **61**:
517 727-45.
518 Jones, A. G., Burger, R. & Arnold, S. J. 2014. Epistasis and natural selection shape the mutational architecture of
519 complex traits. *Nat Commun* **5**: 3709.
520 Kennedy, S. R., Loeb, L. A. & Herr, A. J. 2012. Somatic mutations in aging, cancer and neurodegeneration. *Mech*
521 *Ageing Dev* **133**: 118-26.
522 Kimura, M. 1967. On the evolutionary adjustment of spontaneous mutation rates. *Genetical Research* **9**: 23-34.

523 Loh, E., Salk, J. J. & Loeb, L. A. 2010. Optimization of DNA polymerase mutation rates during bacterial evolution.
524 *Proc Natl Acad Sci U S A* **107**: 1154-9.
525 Lopez-Otin, C., Blasco, M. A., Partridge, L., Serrano, M. & Kroemer, G. 2013. The hallmarks of aging. *Cell* **153**:
526 1194-217.
527 Lotka, A. J. 1925. *Elements of Physical Biology*. Williams and Wilkins.
528 Lynch, M. 2010. Evolution of the mutation rate. *Trends Genet* **26**: 345-52.
529 Lynch, M. 2011. The lower bound to the evolution of mutation rates. *Genome Biol Evol* **3**: 1107-18.
530 Lynch, M., Ackerman, M. S., Gout, J. F., Long, H., Sung, W., Thomas, W. K. & Foster, P. L. 2016. Genetic drift,
531 selection and the evolution of the mutation rate. *Nat Rev Genet* **17**: 704-714.
532 Madsen, T., Arnal, A., Vittecoq, M., Bernex, F., Abadie, J., Labrut, S., Garcia, D., Faugère, D., Lemberger, K. &
533 Beckmann, C. 2017. Cancer Prevalence and Etiology in Wild and Captive Animals. *Ecology and Evolution*
534 *of Cancer*: 11.
535 Marcon, E. & Moens, P. B. 2005. The evolution of meiosis: recruitment and modification of somatic DNA-repair
536 proteins. *Bioessays* **27**: 795-808.
537 Pfau, S. J., Silberman, R. E., Knouse, K. A. & Amon, A. 2016. Aneuploidy impairs hematopoietic stem cell fitness
538 and is selected against in regenerating tissues in vivo. *Genes Dev* **30**: 1395-408.
539 Pothof, J., van Haaften, G., Thijssen, K., Kamath, R. S., Fraser, A. G., Ahringer, J., Plasterk, R. H. & Tijsterman, M.
540 2003. Identification of genes that protect the C. elegans genome against mutations by genome-wide
541 RNAi. *Genes Dev* **17**: 443-8.
542 Rozhok, A. I. & DeGregori, J. 2016. The evolution of lifespan and age-dependent cancer risk. *Trends Cancer* **2**:
543 552-560.
544 Sherr, C. J. 2004. Principles of tumor suppression. *Cell* **116**: 235-46.
545 Sniegowski, P. D., Gerrish, P. J. & Lenski, R. E. 1997. Evolution of high mutation rates in experimental populations
546 of E. coli. *Nature* **387**: 703-5.
547 Swann, J. B. & Smyth, M. J. 2007. Immune surveillance of tumors. *J Clin Invest* **117**: 1137-46.
548 Venditti, C., Meade, A. & Pagel, M. 2011. Multiple routes to mammalian diversity. *Nature* **479**: 393-6.
549 Volterra, V. 1926. Variazioni e fluttuazioni del numero d'individui in specie animali conviventi. *Mem Acad Lincei*
550 *Roma* **2**: 31-113.
551 Williams, G. C. 1966. *Adaptation and Natural Selection: A Critique of Some Current Evolutionary Thought*.
552 Princeton University Press.

553

554

555

556

557 ## Figure legends

558 **Fig. 1. The effect of SMP evolution on the evolution of body mass and mutation rate.** (*A*) physiological/aging
559 related mortality curves generated based on the cumulative distribution function of D_A (Eq. 1). Colors represent the
560 effect of the *Som* (SMP) parameter (Eq. 1). Dotted lines were generated by elevating mutation rate 2-fold. (*B*)
561 modern human mortality in the U.S.A (https://www.ssa.gov). (*C*) evolution of life history traits under positive selection
562 for body size. (*F,G*) population size dynamics when SMP can evolve (corresponds to green in *C-E*) or SMP evolution
563 is blocked (blue in *C-E*); colors indicate individual populations. (*H*) relative frequency of Species B (SMP evolution
564 blocked, blue in *C-E*) in a mixed population with Species A (SMP can evolve, green in *C-E*). For (*C*), (*D*), (*E*) and
565 (*H*) (and similar graphs in other figures), 25 simulations are combined, with the dark line reflecting the mean and
566 shaded area denoting the 95% confidence intervals.

567

568 **Fig. 2. Evolution of body mass, gMR and SMP under various regimens of selection.** Separate experiments are
569 stacked as indicated in their subtitles. The layout: left – body size, middle – gMR, right – SMP (the *Som* parameter
570 in Eq. 1) is maintained as in Fig. 1C-E. Green – the standard condition (as green in Fig. 1C-E); blue – alternative
571 conditions with fixed values of a trait (blue horizontal line in *A,D,F*), when gMR and sMR are dislinked so that the
572 somatic cost is fixed while gMR can evolve (blue in G-I) and under selection for a somatic risk unrelated trait (blue
573 in *J-L*).

574

575 **Fig. 3. The evolution of gMR in in the absence of positive selection for body mass and SMP.** The SMP's *Som*
576 parameter was fixed at 0.34 (red), 0.24 (green; enhanced 10X) and 0.2 (blue; enhanced 40X); a linear decrease in
577 the *Som* value results in a substantially improved SMP, so that the green SMP is ~10X more efficient compared to
578 red, and the blue is a ~4X more efficient SMP than the green. The standard (red) SMP leads to a significantly
579 stronger selection for lower gMR (non-overlapping 95% CIs); however, the absence of difference between the 10X
580 (green) and 40X (blue) improved SMPs indicates that overly improved SMPs might not provide any further
581 difference for how selection acts on gMR.

582

583 **Fig. 4. Positive selection for mutators.** (*A*) frequency of a mutator phenotype in a mixed competitive population
584 with "wild-type" species. Red (1.4X), orange (2X) and green (10X) are mutators of different fold increase in MR
585 relative to the competitor as indicated by the respective numbers. (*B*) positive selection for a somatic cost neutral
586 trait demonstrates faster evolution (and so adaptation) of mutators. Colors and MR fold increase as in (*A*).

587

588 **Fig. 5. A model of how selection acts on mutation rate in sexual populations.** (*A*) under stabilizing selection,
589 the most adaptive phenotypes are close to the population mean/median; such phenotypes are more likely to be
590 produced by parents with low germline mutation rate in a population in which mutation rate is a multi-genic
591 distributed trait. (*B*) under positive selection, the most adaptive phenotypes demonstrate unidirectional deviation of
592 the selected trait(s) from the population mean. Such phenotypes are more likely to be produced by parents having
593 higher germline mutation rate and thus harboring multiple alleles conducive to higher mutation rate; (*C*) small
594 population size reduces the strength of selection by increasing the strength of drift; this condition requires a
595 phenotype to deviate sufficiently far from the population mean/median towards the selected tail to be responsive to
596 selection. Such extremely deviant phenotypes in small populations are likely to come from parents with the highest
597 germline mutation rate and thus harboring fewer alleles for low mutation rate. This condition should impede
598 segregation of mutator alleles from adaptive alleles by recombination imposed by sexual reproduction.

599

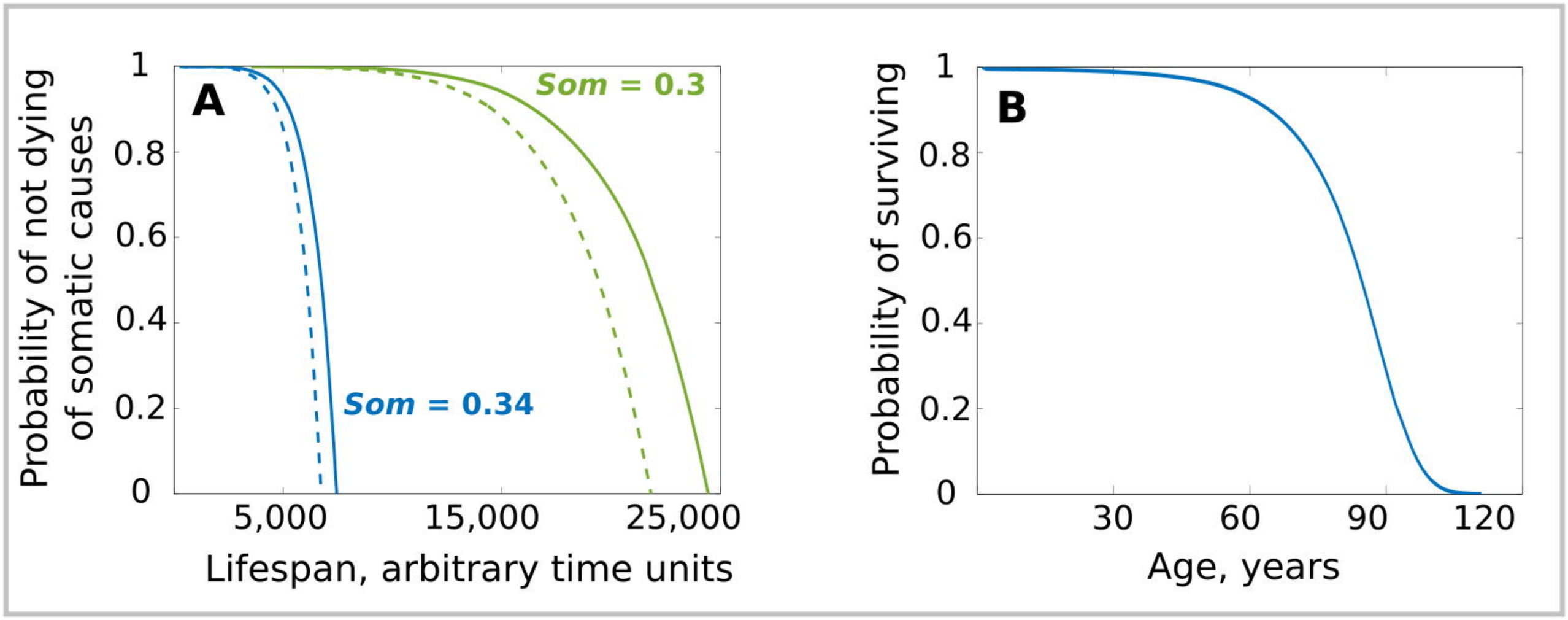
A
Probability of not dying of somatic causes
1
0.8
0.6
0.4
0.2
0
5,000
15,000
25,000
Lifespan, arbitrary time units
Som = 0.3
Som = 0.34
B
Probability of surviving
1
0.8
0.6
0.4
0.2
0
30
60
90
120
Age, years

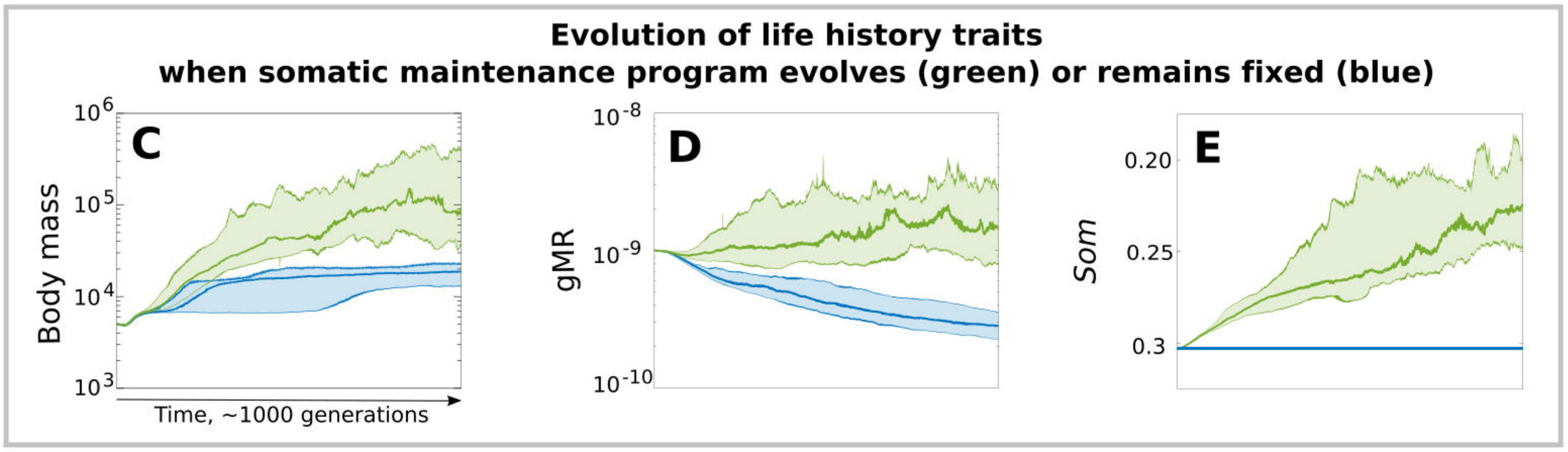
Evolution of life history traits
when somatic maintenance program evolves (green) or remains fixed (blue)
C
Body mass
10^6
10^5
10^4
10^3
Time, ~1000 generations
D
gMR
10^{-8}
10^{-9}
10^{-10}
E
Som
0.20
0.25
0.3

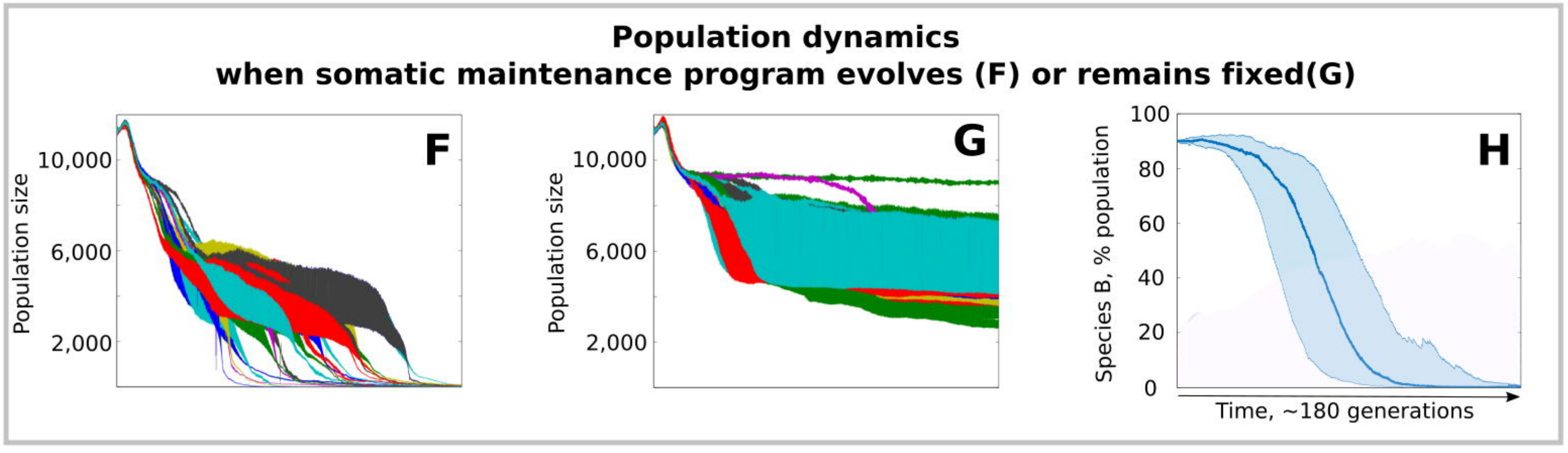
Population dynamics
when somatic maintenance program evolves (F) or remains fixed(G)
F
Population size
10,000
6,000
2,000
G
Population size
10,000
6,000
2,000
H
Species B, % population
100
80
60
40
20
0
Time, ~180 generations

Evolution of mutation rate (B) and somatic maintenance (C) when body mass is evolving (A, green) or remains fixed (A, blue)

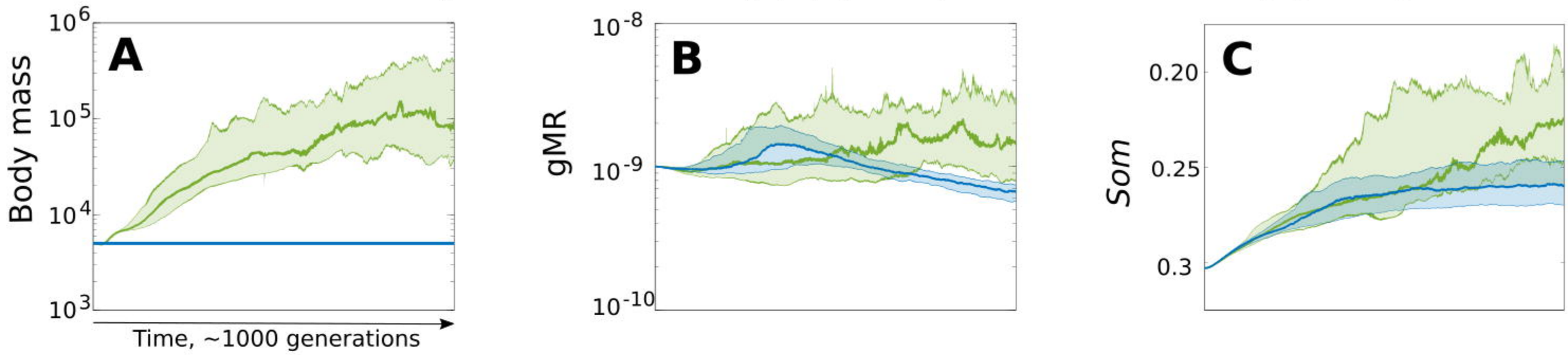

Evolution of mutation rate (E) when body mass and somatic maintenance are evolving (A, F, green) or remain fixed (A, F, blue)

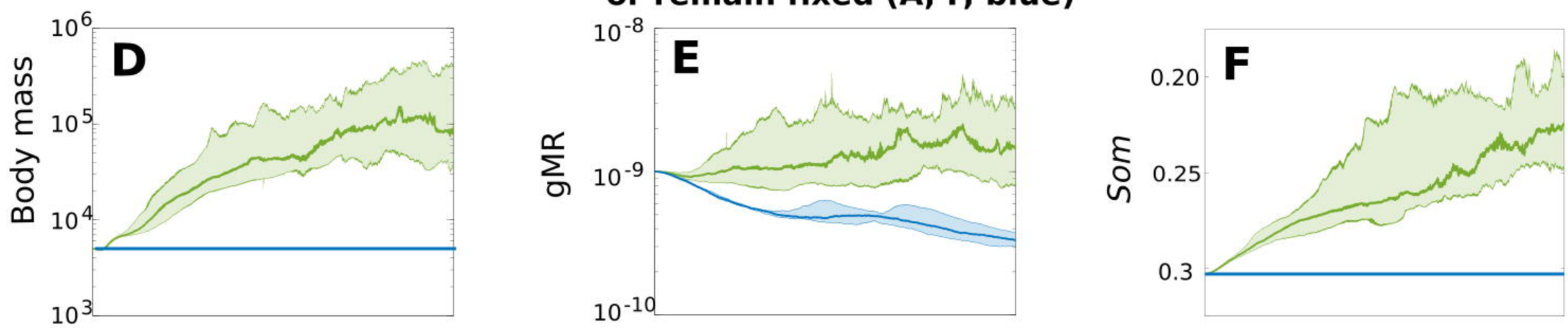

Evolution of life history traits when somatic and germline mutation rates, MR, are linked (green) or somatic MR remains fixed while germline MR evolves (blue)

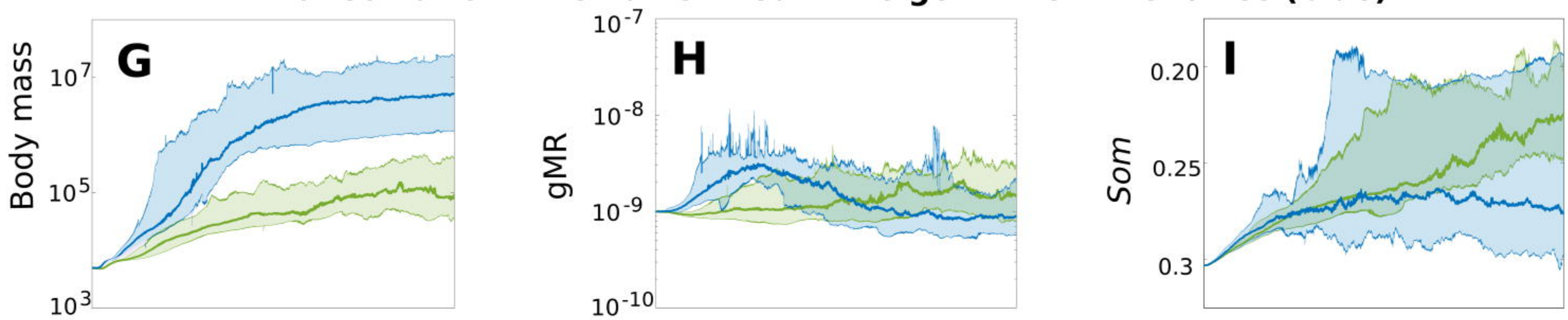

Evolution of mutation rate (K) and somatic maintenance (L) under positive selection for body size (J, green) or somatic risk unrelated trait (J, blue)

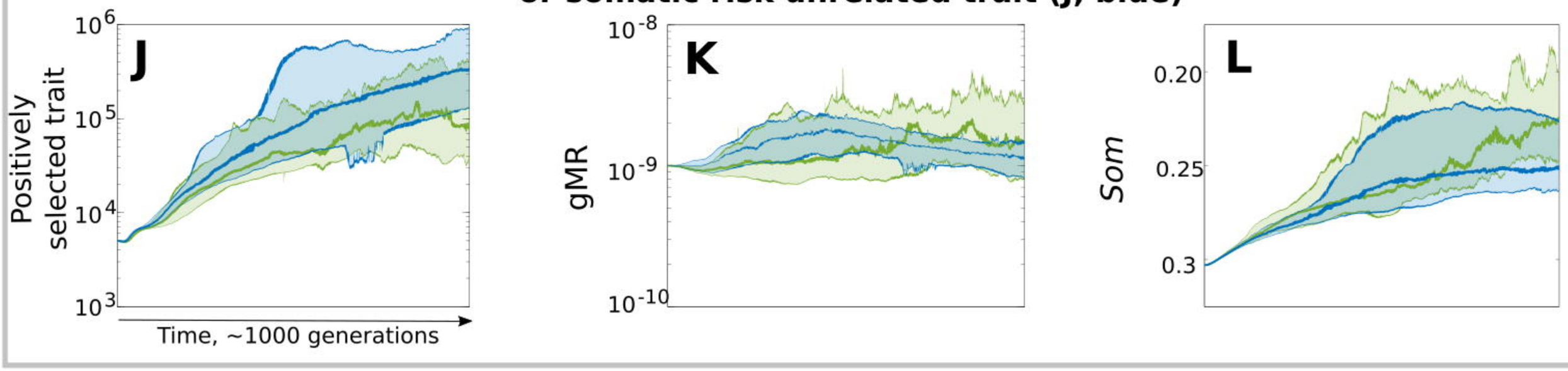

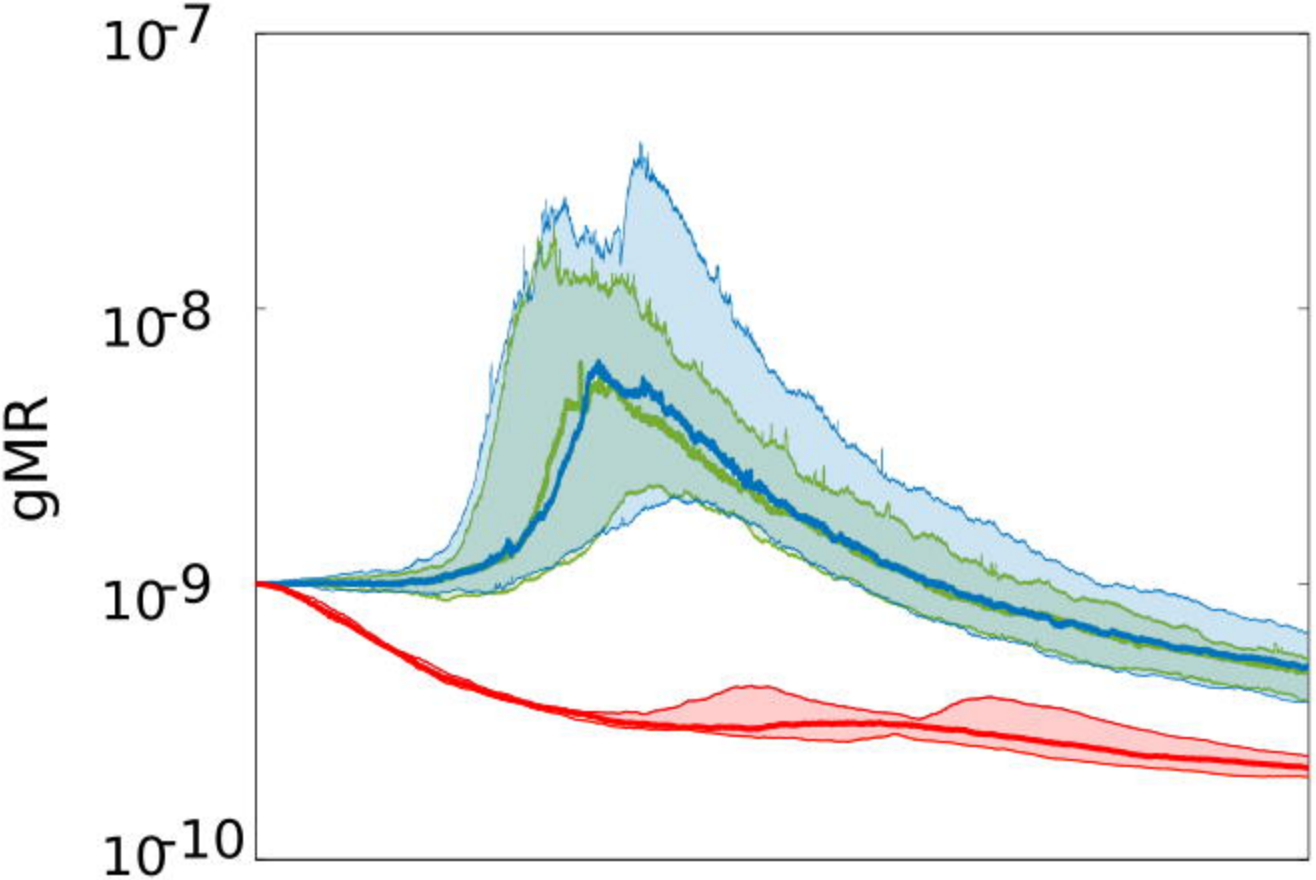
10^{-7}
10^{-8}
10^{-9}
10^{-10}
gMR

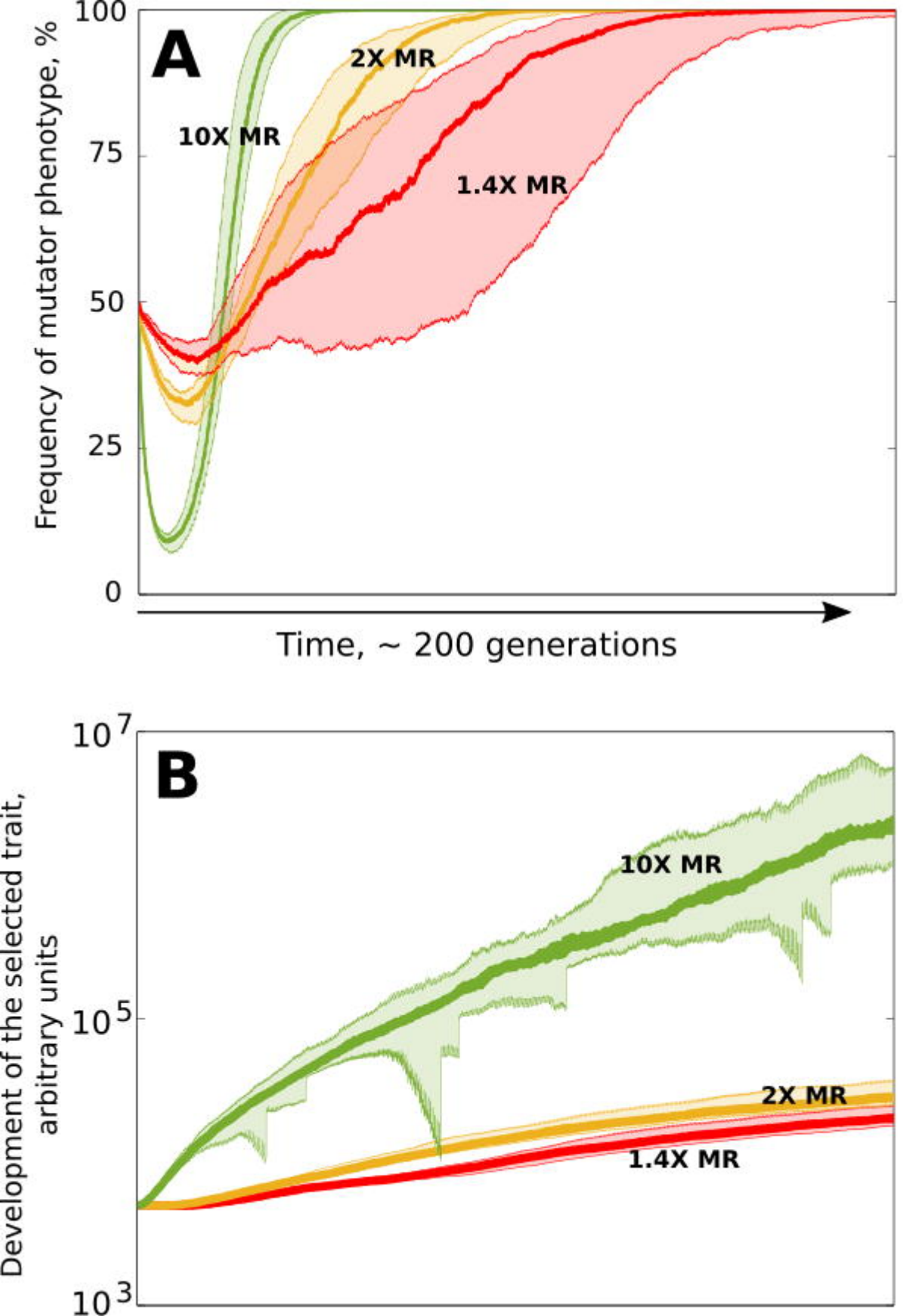
A
100
75
50
25
0
Frequency of mutator phenotype, %
10X MR
2X MR
1.4X MR
Time, ~ 200 generations
B
10^7
10^5
10^3
Development of the selected trait, arbitrary units
10X MR
2X MR
1.4X MR

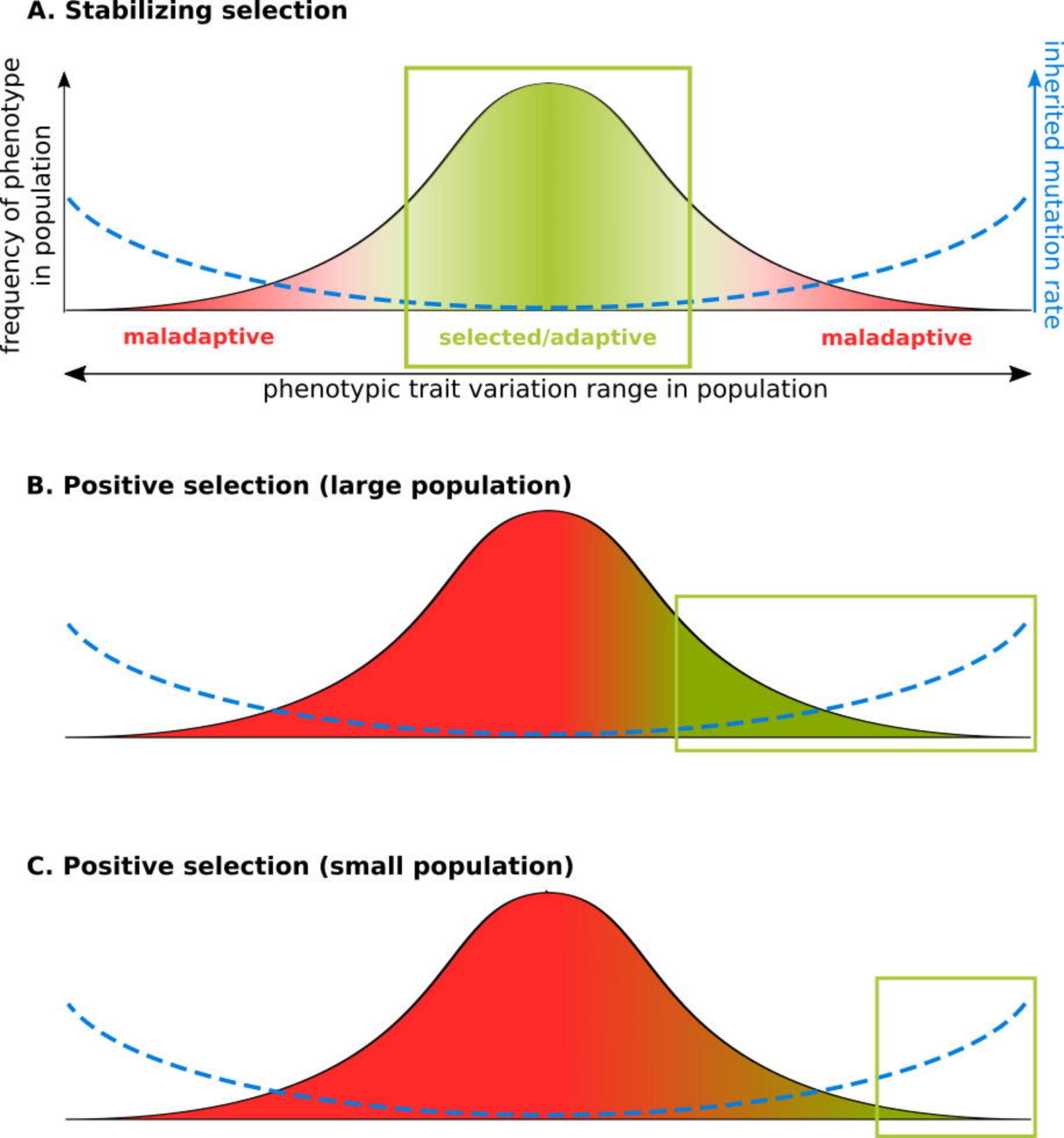
A. Stabilizing selection
frequency of phenotype in population
inherited mutation rate
maladaptive
selected/adaptive
maladaptive
phenotypic trait variation range in population
B. Positive selection (large population)
C. Positive selection (small population)